


## ORIGINAL RESEARCH PAPER

# *RYR2* mutation in non-small cell lung cancer prolongs survival via down-regulation of *DKK1* and up-regulation of *GS1-115G20.1*: A weighted gene Co-expression network analysis and risk prognostic models

Wenjun Ren<sup>1,2,3,4</sup>  | Yongwu Li<sup>3,4</sup> | Xi Chen<sup>2,5</sup> | Sheng Hu<sup>2,6</sup> | Wanli Cheng<sup>1,2</sup> | Yu Cao<sup>3,4</sup> | Jingcheng Gao<sup>3,4</sup> | Xia Chen<sup>3,4</sup> | Da Xiong<sup>3,4</sup> | Hongrong Li<sup>3,4</sup> | Ping Wang<sup>1,2</sup>

<sup>1</sup>Department of Thoracic Surgery, The Second Affiliated Hospital of Kunming Medical University, Kunming, China

<sup>2</sup>Kunming Medical University, Kunming, Yunnan, China

<sup>3</sup>Department of Cardiovascular Surgery, The First People's Hospital of Yunnan Province, Kunming, China

<sup>4</sup>Department of Cardiovascular Surgery, Affiliated Hospital of Kunming University of Science and Technology, Kunming, China

<sup>5</sup>First Department of Neurosurgery, The Second Affiliated Hospital of Kunming Medical University, Kunming, China

<sup>6</sup>Second Department of Hepatobiliary Surgery, The Second Affiliated Hospital of Kunming Medical University, Kunming, China

## Correspondence

Ping Wang, Department of Thoracic Surgery, The Second Affiliated Hospital of Kunming Medical University, Kunming, 650101, China.

Email: wangping2467@126.com

## Funding information

the Open Project of The First People's Hospital of Yunnan Province Clinical Medicine Center, Grant/Award Number: 2021LCZXXF-XZ03; the Applied Basic Research Project of Yunnan provincial Science and Technology Department and Kunming Medical University, Grant/Award Numbers:

202001AY070001-117, 202001AY070001-130,

202001AY070001-284

## Abstract

*RYR2* mutation is clinically frequent in non-small cell lung cancer (NSCLC) with its function being elusive. We downloaded lung squamous cell carcinoma and lung adenocarcinoma samples from the TCGA database, split the samples into *RYR2* mutant group ( $n = 337$ ) and *RYR2* wild group ( $n = 634$ ), and established Kaplan-Meier curves. The results showed that *RYR2* mutant group lived longer than the wild group ( $p = 0.027$ ). Weighted gene co-expression network analysis (WGCNA) of differentially expressed genes (DEGs) yielded prognosis-related genes. Five mRNAs and 10 lncRNAs were selected to build survival prognostic models with other clinical features. The AUCs of 2 models are 0.622 and 0.565 for predicting survival at 3 years. Among these genes, the AUCs of *DKK1* and *GS1-115G20.1* expression levels were 0.607 and 0.560, respectively, which predicted the 3-year survival rate of NSCLC sufferers. GSEA identified an association of high *DKK1* expression with *TP53*, *MTOR*, and *VEGF* expression. Several target miRNAs interacting with *GS1-115G20.1* were observed to show the relationship with the phenotype, treatment, and survival of NSCLC. NSCLC patients with *RYR2* mutation may obtain better prognosis by down-regulating *DKK1* and up-regulating *GS1-115G20.1*.

## KEYWORDS

Dickkopf Wnt signalling pathway inhibitor-1, differentially expressed gene, long non-coding RNA, non-small cell lung cancer, prognostic signature, ryanodine receptor 2

Wenjun Ren and Yongwu Li contributed equally.

This is an open access article under the terms of the Creative Commons Attribution-NonCommercial-NoDerivs License, which permits use and distribution in any medium, provided the original work is properly cited, the use is non-commercial and no modifications or adaptations are made.

© 2021 The Authors. *IET Systems Biology* published by John Wiley & Sons Ltd on behalf of The Institution of Engineering and Technology.

## 1 | INTRODUCTION

Globally, the number of lung cancer cases and deaths is increasing, with GLOBOCAN statistics in 2018 showing approximately more than 2 million new cases of lung cancer, reported to hold 11.6% of all cancer types, and 1.76 million deaths, accounting for 18% of all cancers [1]. Despite the availability of surgery, chemotherapy, and targeted drug therapy [2], the overall survival (OS) of lung cancer is still disappointing, with a survival rate at 5 years of only 19.4% [3]. Non-small cell lung cancer (NSCLC) is the highest prevalent subtype reported to take up 85% of total lung cancers [4]. Depending on the different pathological features, NSCLC can be further classified into three types: squamous cell carcinoma, adenocarcinoma, and large cell carcinoma. In NSCLC cells, there are a large number of genetic and epigenetic alterations [5], which have an important impact on the pathogenesis and progression of NSCLC. Understanding the somatic genetic mutations and transcriptome changes of NSCLC is of great significance for improving the prognosis of NSCLC.

Many cancer genetic studies have identified frequent mutations in the genes that encode extremely large protein molecules in cancer cells, and these mutated genes include *TTN*, *RYR2*, *RYR3*, *MUC16*, *MUC4*, and *DNAH5* [6]. In order to study human cancers at the gene and transcriptional product level, numerous public databases from large patient cohorts have been created to identify various biomarkers related to cancer pathogenesis, progression and therapeutic responses [7, 8]. By analysing public data, we found that *RYR2* mutation is a clinically frequent variant in NSCLC. Ryanodine receptor two protein, encoded by the *RYR2* gene, is predominantly distributed in heart and involved in excitation–contraction coupling [9], whose mutations are mainly associated with a range of myopathies and arrhythmias [10]. Although *RYR2* polymorphisms have been confirmed for underlying functions in three different regions or “hot-spots” of the coding sequence, the study of its assumed function in cancers is still in its initial stages and further studies are expected [11]. Schmitt, K et al. found differential promoter methylation status and expression level of *RYR2* in head and neck tumor, suggesting that reduced expression of *RYR2* in adjacent tissues and precancerous lesions may potentially indicate poor survival and impending malignancy [6]. In oesophageal cancer, the *RYR2* mutation upregulated signalling pathways involved in the immune response and enhanced anti-tumor immunity [12]. The *RYR2* rs12594 mutation (occurring in the 3'-UTR) also significantly reduced the risk of developing breast cancer [13]. Nevertheless, its role in NSCLC is currently unknown.

Long non-coding RNAs (lncRNAs), a type of RNA molecule composed of over 200 nucleotides, are structurally similar to messenger RNAs but not translated into proteins [14, 15]. The main ways in which lncRNAs perform biological functions in disease include: RNA decoy, miRNA sponge, constituting RNP, recruiting chromatin modifier as

well as influencing transcription, splicing and degradation of mRNA [16]. More and more evidences have shown that lncRNAs are disordered in human cancer [17]. Yang et al. demonstrated that NSCLC cells with up-regulated lncRNA *GACAT3* expression have increased the resistance of tumor cells to radiotherapy [18], while Shi's group uncovered that down-regulated *GAS5* expression in NSCLC suggested poor prognosis [19]. Although there is no lncRNA specifically associated with NSCLC, the crucial functions which lncRNAs play towards the diagnosis, treatment and prognostic evaluation of NSCLC are emerging [16].

In this study, we used a series of bioinformatical tools to construct risk prognostic models of mRNAs and lncRNAs in NSCLC with *RYR2* mutations. For the first time, significant associations of high *DKK1* or low *GSI-115G20.1* expressions with the poor outcomes of NSCLC in the presence of *RYR2* mutations were uncovered, and a significant negative correlation was identified between the expression of *DKK1* and *GSI-115G20.1* in *RYR2* mutated NSCLC.

## 2 | MATERIALS AND METHODS

### 2.1 | Sample preparation and preprocessing

Genomic and transcriptomic data was retrieved from the lung adenocarcinoma (LUAD) and lung squamous cell carcinoma (LUSC) files which are documented in the Cancer Genome Atlas (TCGA) on the UCSC Xena platform (<https://xenabrowser.net/>). Samples with no survival status or survival time were removed from our study, while the samples with both genomic and transcriptomic data were retained. According to the mutation data detected by the Varscan2 software [20], those containing *RYR2* sense mutations were classified as the mutant group, while those without *RYR2* sense mutations were classified as the wild group. We used Kaplan-Meier curves to analyse survival differences between the *RYR2* mutant and wild groups and included age, gender, TNM classification of the tumour, disease diagnosis (LUAD or LUSC) and tumour stage as covariates to reduce the effect of confounding factors.

### 2.2 | Identification of differentially expressed genes (DEGs) and functional enrichment analysis

Differentially expressed mRNAs (DEmRNAs) and lncRNAs (DElncRNAs) were analysed by R package “edgeR” between the *RYR2* mutant group ( $n = 337$ ) and *RYR2* wild group ( $n = 634$ ), the DEmRNAs and DElncRNAs with adjusted p values less than 0.05 were retained [21, 22]. Gene Ontology (GO) analysis [23, 24] and Kyoto Encyclopaedia of Genes and Genomes (KEGG) pathway enrichment analysis were run for differential mRNAs with R package “clusterProfiler” [24].

## 2.3 | Weighted gene co-expression network analysis (WGCNA)

The modules of co-expressed differential mRNAs and lncRNAs were identified by R package “WGCNA” [25, 26]. First, a suitable soft threshold  $\beta = 6$  was calculated. Then, average linkage hierarchical clustering was realised on a dendrogram as a result of DynamicTreeCut analysis based on a Topological Overlap Measure (TOM)-based dissimilarity matrix. A minimum threshold of 40 was set to group the genes of similar expression pattern into the same modules. Module eigengenes (MEs) were calculated, and then the modules were analysed by clustering, and the closer modules were merged into new modules by setting height = 0.5. To determine the association with clinical traits, gene significance (GS) for each module was computed, and higher GS indicated genes with more biologically significant association with clinical features. Module-gene significance (MS) describes the relationship between module gene expression profiles and MEs. Then, MEs were correlated with different clinical features to identify the modules associated with prognosis [27].

## 2.4 | Risk prognostic model based on multivariate COX proportional hazard model

For DEGs, univariate regression analysis with  $p < 0.05$  was used as a filter to identify prognosis-related mRNAs and lncRNAs by combining clinical information. The mRNA genes and lncRNA genes associated with prognosis were screened by the least absolute shrinkage and selection operator (Lasso) Cox penalised regression model. Corresponding coefficients were obtained, and risk prognostic models of the identified mRNAs and lncRNAs were constructed according to the expression levels and coefficients of these genes. According to the models, each patient was scored and then defined as high and low risk by taking the median score as the threshold. Differences in survival rates between the two cohorts were analysed. Time-dependent receiver operating characteristic (ROC) curves were drawn to determine the predictive performance of risk score one and risk score two on the survival of NSCLC patients at 3 years. To further investigate the reliability of the mRNA prediction model, we downloaded the data of the other article for external validation of the 3-year survival rate [28].

## 2.5 | Analysis of crucial DEmRNA *DKK1* and DELncRNA *GS1-115G20.1*

Multivariate Cox regression models were constructed to validate whether the crucial DEmRNA *DKK1* and DELncRNA *GS1-115G20.1* are prognostic factors independent of other clinical factors. Statistical significance was defined when  $p < 0.05$ . According to *TP53* mutation, the samples were split into the *TP53* mutant group and wild group. Thereafter,

expressions of *DKK1* and *GS1-115G20.1* in both groups were compared. Median expression-based grouping was then performed to classify patients into high and low expression groups, and Kaplan-Meier curves were plotted to compare their survival. ROC analysis was run to evaluate the predictive accuracy of *DKK1* and *GS1-115G20.1* on 3-year survival in NSCLC.

The transcriptomic data were processed by GSEA software based on the high and low *DKK1* expression in the samples [29]. The DEGs between the high and low expression groups of *DKK1* were analysed by the R package “edgeR”, and then the DEGs list was annotated by DAVID [30]. To identify the transcription factors (TFs), the DEGs in high and low *DKK1* expression groups were analysed by R package “edgeR”, and a total of 1485 DEGs were obtained with the condition that  $p < 0.05$  and  $|\log_2(\text{FC})| \geq 0.8$ . The list of DEGs was annotated by DAVID (module UCSC\_TFBS of function Protein-Interactions), and the filtering condition was  $p < 0.05$ . In this way, we can use the UCSC database collection of TFBS (transcription factor binding sites) to understand which transcription factors the genes are enriched to.

To further investigate DELncRNA *GS1-115G20.1*, we used the StarBase v2.0 database [31] for the competing endogenous RNAs (ceRNAs) of *C1ORF21*, which took the top 20. The correlation of *C1ORF21*, *GS1-115G20.1* and ceRNAs expression was performed separately based on the data obtained from this analysis. The Custom Prediction function of the miRDB database (<http://www.mirdb.org/>) was consulted to show the possible miRNA targets of *GS1-115G20.1* [32].

## 2.6 | Ethical statement

Not applicable.

## 2.7 | Statistical analysis

Statistical tests and plots were completed on R and GraphPad Prism 7.04. A difference of statistical significance was defined at  $p < 0.05$ . In the graph,  $*p < 0.05$ ,  $**p < 0.01$ ,  $***p < 0.001$ ,  $****p < 0.0001$ .

## 3 | RESULTS

### 3.1 | Survival analysis of the *RYR2* mutant group and wild group

Figure 1 shows the workflow of the whole study. Totally, 971 analysable NSCLC samples were obtained by the UCSC Xena database retrieval (Table S1), which were split into the *RYR2* mutant group ( $n = 337$ ) and the wild group ( $n = 634$ ) (Table 1). See Table S2 for a comparison of the clinical characteristics of the two groups of patients. Between-group comparison for survival was implemented, and it was

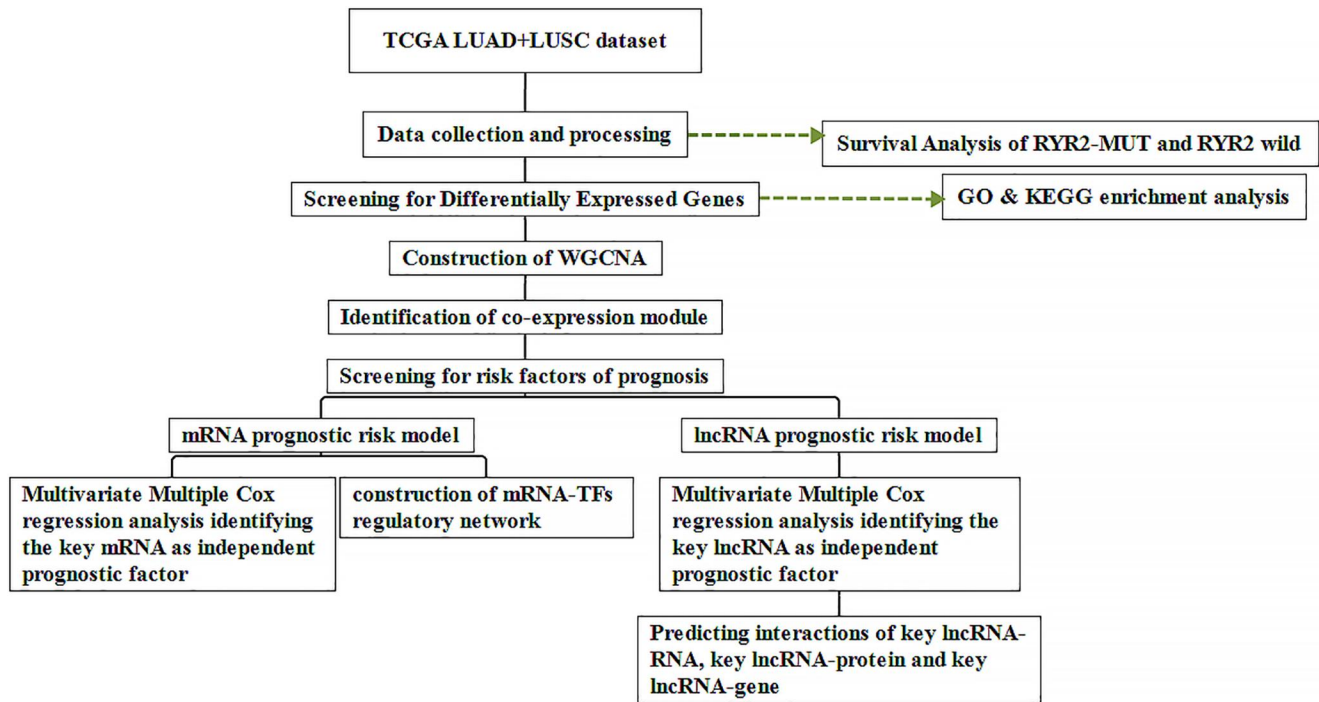


FIGURE 1 Workflow chart of the study

TABLE 1 NSCLC samples based on *RYR2* mutation/wild grouping

	No. of pts.	<i>RYR2</i> MUT	<i>RYR2</i> WT
LUAD	491	171	320
LUSC	480	166	314

Abbreviations: NSCLC, non-small cell lung cancer; LUAD, lung adenocarcinoma; LUSC, lung squamous cancer; pts, patients; MUT, mutation; WT, wild type.

demonstrated that the OS of the *RYR2* mutant group was longer than that of the *RYR2* wild group (HR = 0.778 95% CI = 0.625–0.969) (Figure 2a), with the statistical significance as indicated in the logarithmic rank test ( $p = 0.025$ ).

### 3.2 | DEmRNAs and DElncRNAs between the *RYR2* mutant group and wild group

The DEmRNAs and DElncRNAs between the *RYR2* mutation and wild group were screened by using R package “edgeR” on 971 patients genomic and transcriptomic data. With  $p < 0.05$ , 9271 DEGs were obtained in total, composed of 5346 DEmRNAs and 3925 DElncRNAs (Table 2). Compared with the wild group, the mutant group had 2702 up-regulated and 2644 down-regulated mRNAs, with significantly reduced transcription of *RYR2* ( $\log_{2}FC = -0.376$   $p = 4.43e-4$ ) (Figures 2b,c, Table S3); besides, 2168 and 1857 lncRNAs were differentially up-regulated and down-regulated, respectively, in the mutant group (Figures 2d,e, Table S4).

Functional enrichment analysis of DEmRNAs was performed by R package “clusterProfiler”. GO annotation showed that DEmRNAs were mainly associated with nuclear division,

organelle division, transmembrane transport complex, and metal ion transmembrane transport activity (Figure 3a–c, Table S5). Additionally, KEGG pathway enrichment analysis revealed that the genes of DEmRNA were predominantly involved in neuroactive ligand-receptor interaction, complement and coagulation cascades, cAMP signalling pathway, adrenergic signalling in cardiomyocytes, cell cycle and other pathways (Figure 3d, Table S6).

### 3.3 | Construction of co-expression network to identify prognosis-related modules

DEmRNAs and DElncRNAs were projected onto a weighted co-expression network with the R package “WGCNA”, and then the modules obtained were clustered into 24 modules in total (Figure 4a), with the module sizes ranging from 52 to 2208 genes (Table 3). Independent genes were clustered into grey modules which were excluded from this analysis. The topological overlap of co-expressed genes in each module was shown in the DEGs heat map (Figure 4b), and the relationship of the 24 co-expression modules was shown in the eigengene adjacency heat map (Figure 4c). Pearson correlation coefficients were calculated for the MEs. The numbers displayed in each small cell are the coefficients that reflect the association between the gene modules and the corresponding clinical factors, and the numbers in parentheses indicate the  $p$ -value. In Figure 4d, we can conclude significant associations of the blue and light green modules with one-year survival and the red module with OS; hence, genes from these three modules were selected for further analysis.

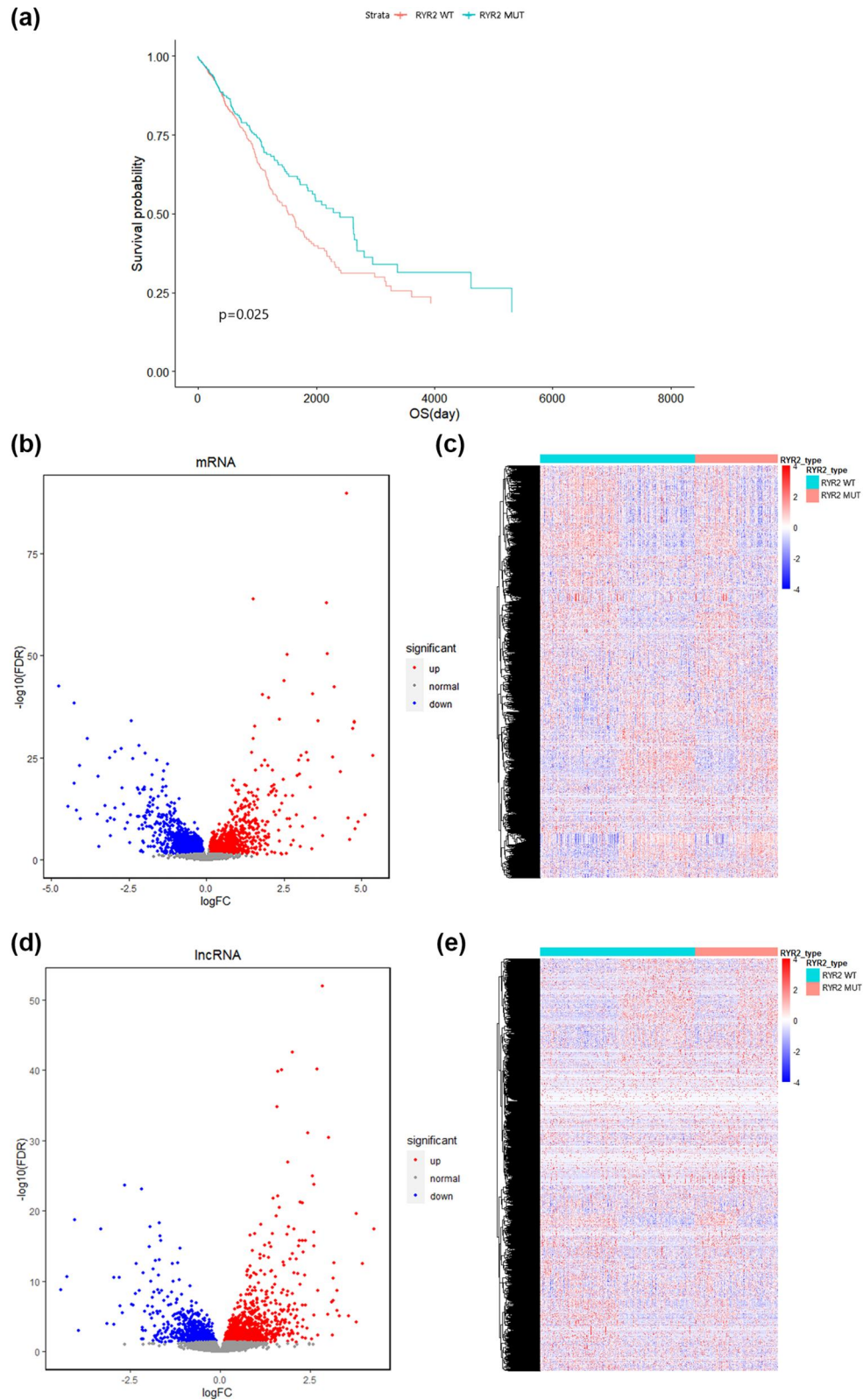


**FIGURE 2** Overall survival and DEGs of RYR2 mutant group and wild group. (a) Kaplan-Meier curve comparison of survival times between RYR2 wild-type and mutant groups. (b, c) volcano plot (b) and heat map (c) of DEmRNAs obtained by “edgeR” analysis. (d, e): volcano plot (d) and heat map (e) of DElncRNAs obtained by “edgeR” analysis. DEGs, differentially expressed genes; DElncRNAs, differentially expressed lncRNAs; DEmRNAs, differentially expressed mRNAs; FC, fold change; FDR, false discovery rate; RYR2 WT, RYR2 wild-type; RYR2 MUT, RYR2 mutant

### 3.4 | Univariate regression analysis to screen prognosis-related genes in blue, light green, and red modules

For DEGs, univariate regression analysis with  $p < 0.05$  as the filtering condition was used to screen a total of 77 prognosis-related genes from blue, light green and red modules, including 57 mRNAs and 20 lncRNAs (Table S7), and the significance was selected for forest plotting from the top 15 (Figure 5a). With the median expression of prognosis-related genes in all samples considered, the samples were grouped into high and low expression cohorts, and survival conditions were analysed using R package “survival”. Among them, 13 genes were differentially expressed with statistically significant differences in OS, and the Kaplan-Meier curves were shown (Figure 5b–e and Figure S1).

### 3.5 | Risk prognostic model of mRNA

The 57 prognosis-related mRNAs obtained by univariate regression analysis were put into a Lasso regression model, and

12 mRNAs were selected according to the parameter Lambda value, with Lambda.min. The minimum value was used as the threshold (Figures S2a–b), and then the Cox penalty regression model was used to reduce the dimension and finally screened a linear risk score model consisting of 5 mRNA genes associated with survival: risk score 1 =  $\sum$  (coefficient \* expression level of mRNA) =  $(-4.27e-3 * RAB44) + (-5.11e-4 * GNG7) + (1.61e-4 * RASA3) + (-1.26e-3 * CD200R1) + (3.69e-5 * DKK1)$ .

All samples were assigned a score and defined as high- and low risk based on the median risk score 1 value as the cutoff. Figure 6a shows the expression of 5 prognosis-related mRNAs in two cohorts. Figure 6b shows the survival time in two groups, and Figure 6c shows the heat map which reflects the expression of the 5 genes in the risk model in different risk score 1, diagnoses, and genders. The Kaplan-Meier curve shows the lower OS of the high-risk patients compared with the low-risk group (Figure 6d); meanwhile, the area under the ROC curve (AUC) for the survival rate at 3 years was 0.622, indicating the favourable predictive ability of the risk model (Figure 6e).

Risk score 1 was combined with the age, gender, tumour stage, presence of *EGFR* mutation, type of diagnosed disease, smoking history, tumour location, and clinical factors of radiation therapy in a multivariate Cox regression model. Age, tumour stage, radiation therapy and risk score 1 were determined as independent predictive factors for OS, while risk score 1 possessed a stronger impact on survival (Figure 6f). In order to facilitate the utilisation of risk score 1, a nomogram

TABLE 2 Differentially expressed mRNAs and lncRNAs

	DEGs	Up	Down
mRNA	5346	2702	2644
lncRNA	3925	2168	1757

Abbreviation: DEGs, differentially expressed genes.

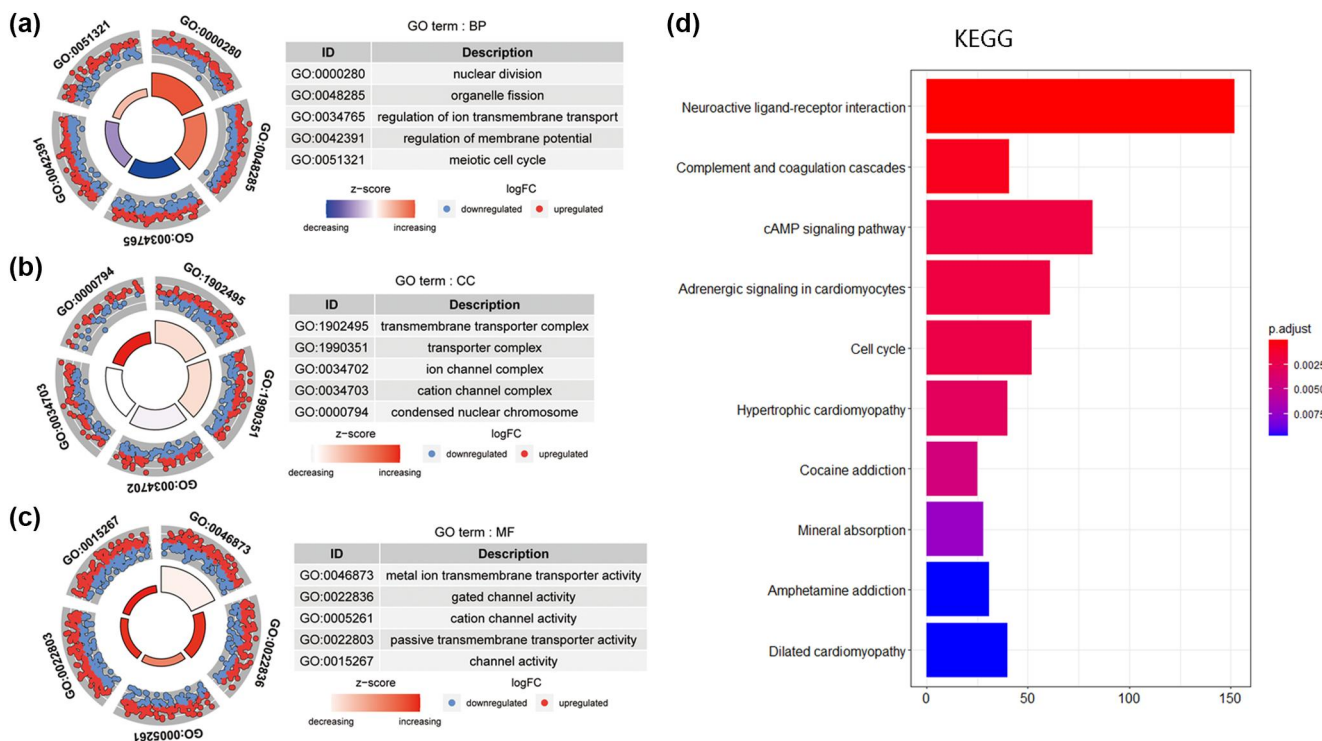
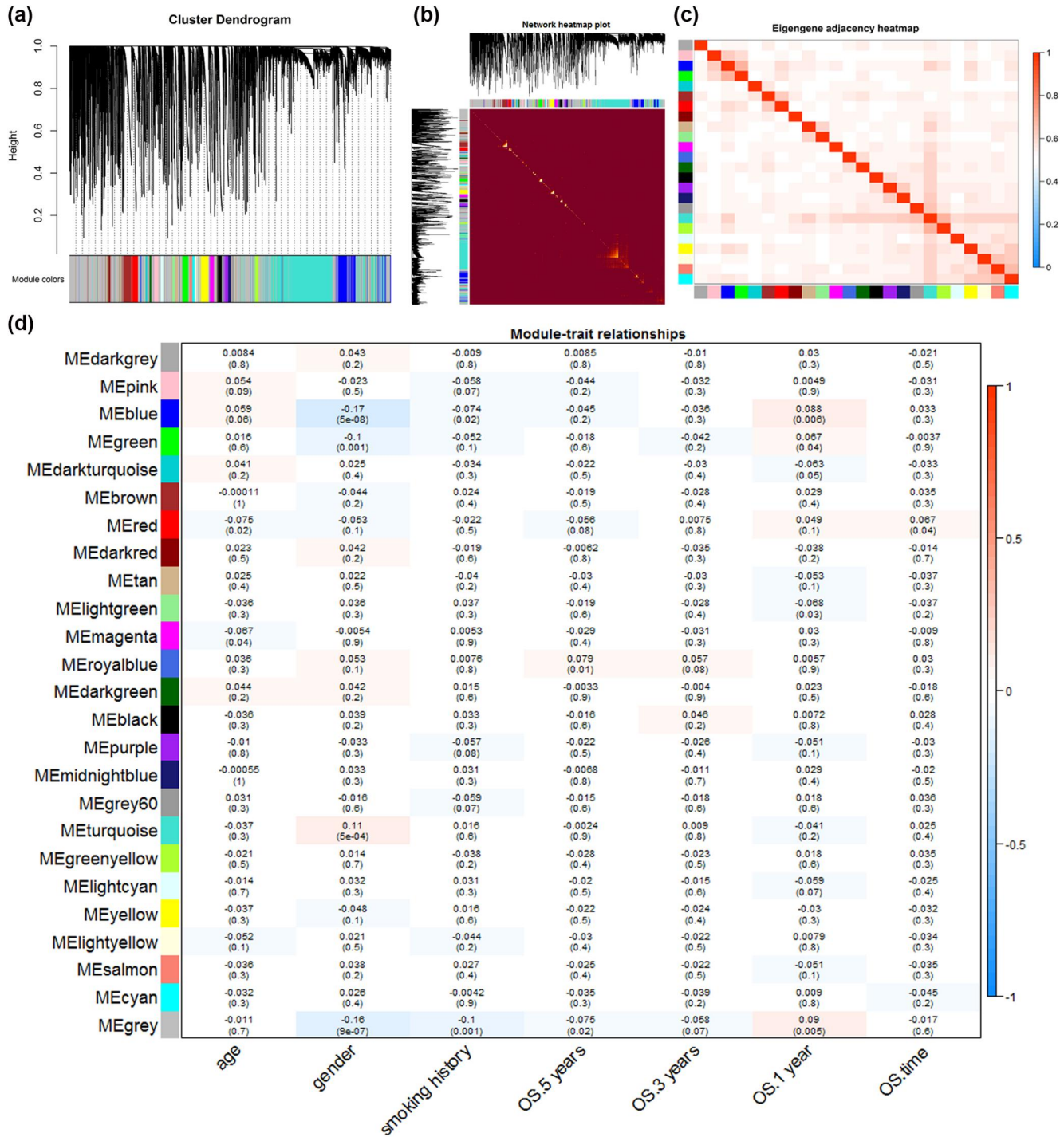


FIGURE 3 The most enriched GO terms and KEGG pathways of DEmRNA. (a, b, c) GO functional enrichment analysis annotated DEmRNA in terms of BP (a), CC (b), and MF (c), respectively. (d) KEGG pathway analysis. The X-axis displays the number of genes activated in each pathway. BP, biological process; CC, cellular component; KEGG, Kyoto encyclopaedia of genes and genomes; MF, molecular function



**FIGURE 4** Network construction and module-trait relationships of co-expressed genes. (a) Clustered dendrograms and co-expression network modules generated by topologically overlapping DEGs based on average linkage hierarchical clustering. Each branch in the tree diagram represents a gene. Euclidean distances are highly depicted. Each colour indicates a different co-expression module. (b) Heat map of topological overlap. Yellow areas represent high levels of topological overlap. (c) Heat map of feature gene adjacency. The heat map shows the correlation between different co-expression modules. (d) Module-trait relationship. Each row is a specific module and each column is a clinical feature. The  $R^2$  and  $p$  values (in parentheses) for the Pearson correlations of modules with clinical traits were shown in the squares. Gradient colour ranging from  $-1$  to  $1$  represent the  $R^2$ -values of Pearson correlations. ME, module eigengene; OS, overall survival

was plotted (Figure 6g). The results of the external validation showed that the area under the ROC curve for 3 year survival had an AUC of 0.595 and this model had acceptable predictive power (Figure S3).

### 3.6 | Risk prognostic model of lncRNA

The 20 lncRNAs with prognostic related genes obtained by univariate regression analysis were first analysed by Lasso

**TABLE 3** Gene number of each WGCNA module

Module	No. of genes	Module	No. of genes
Black	145	Light green	71
Blue	596	Light yellow	69
Brown	290	Magenta	134
Cyan	98	Midnight blue	93
Dark green	59	Pink	137
Dark grey	52	Purple	129
Dark red	64	Red	189
Dark turquoise	53	Royal blue	67
Green	196	Salmon	106
Green yellow	113	Tan	112
Grey	72	Turquoise	2208
Light cyan	74	Yellow	275

regression analysis (Figures S2c–d), and 10 lncRNAs were selected by the threshold parameter, Lambda.min (Figure 7a), which constitutes a linear risk assessment model associated with survival. The lncRNA risk score model is risk score 2 =  $\sum$  (coefficient \* expression level of lncRNA) =  $(-3.86e-4*LI\ NC00402) + (-7.83e-3*AC007880.1) + (-1.74e-3*LINC013\ 52) + (-7.58e-4*RP11-354E11.2) + (-3.28e-3*RP11-374F3.5) + (-6.46e-4*AC018647.3) + (-5.75e-4*HLA-DQB1-AS1) + (-3.45e-2*GS1-115G20.1) + (-4.34e-3*SMCR5) + (-2.00e-3*RP11-357N13.6)$ .

Similarly, all samples were assigned into high- and low-risk cohorts (cutoff: risk score 2). Figure 7b demonstrates the change in risk values; Figure 7c demonstrates the survival difference; Figure 7d carries out the expression of 10 genes in the two cohorts, the diagnostic outcome, and the gender subgroup. Survival curves (Figure 7e) indicated that the OS rate of patients with high-risk was lower; meanwhile, the AUC value was 0.565, suggesting that the model had certain predictive accuracy in the prognosis of NSCLC patients (Figure 7f).

Risk score 2 was combined with the age, gender, tumour stage, presence of *EGFR* mutation, types of diagnosed disease, smoking history, tumour location, and clinical factors of radiation therapy in a multivariate Cox regression analysis. Age, tumour stage, radiation therapy and risk score two were observed to be the predictive factors for OS in an independent manner, while the prognostic performance of risk score two was much greater (Figure 7g). Similarly, the nomogram was plotted (Figure 7h).

### 3.7 | Crucial prognosis-related mRNA gene *DKK1* is an independent prognostic factor and correlated with the expression of *TP53*, *MTOR*, *VEGF*

The mRNA genes included in the risk score 1 were analysed. There were five mRNA genes in the mRNA-based risk

prognostic model, and only one gene, *DKK1*, was carried out with survival significance between high and low expression groups (Figure 5b). *DKK1*, therefore, was selected for the study and then observed to present increased expression in the TP53 mutation group compared with the wild group with a statistically significant difference (Figure 8a). The AUC value was 0.607 using high and low *DKK1* expressions to predict survival at 3 years of NSCLC cases (Figure 8b). With clinical information considered, multivariate analysis by Cox regression identified *DKK1* as an independent prognostic factor (Figure 8c). Additionally, GSEA analysis found that the differential genes in the high and the low *DKK1* expression groups were related to the expression of *mTOR*, *VEGF* and *TP53* (Figure 8d).

With regard to the regulation network of mRNA-TFs, 911 DEGs were of decreased expression and 574 DEGs were of increased expression (Table S8). The DEGs which were enriched in these TFs were: CHX10, S8, E47, LHX3, CREL, AP1 and HNF3B. The top 18 TFs associated mRNAs with greater  $|\log_2(FC)|$  were selected for the regulatory network mapping (Figure 9).

### 3.8 | Crucial prognosis-related lncRNA *GS1-115G20.1* is an independent prognostic factor, associated with the expression of *C1ORF21*, multiple target miRNAs, and *DKK1*

The lncRNA genes in the risk score 2 were analysed, and the patients were assigned into high and low expression groups on the basis of median lncRNA expression values. *GS1-115G20.1* was identified to be of survival significance at a higher degree (Figure 5c); *GS1-115G20.1*, therefore, was selected for the study. *TP53* mutation group witnessed a downward trend of *GS1-115G20.1* expression compared with the wild group characterised by a statistically significant difference (Figure 10a). The expression level of *GS1-115G20.1* was used to predict the 3 year survival rate of NSCLC cases with AUC = 0.560 (Figure 10b). Combined with the clinical information, multivariate Cox regression analysis showed that *GS1-115G20.1* was a prognostic factor independent of other variables (Figure 10c).

The correlation analysis by *C1ORF21*, *GS1-115G20.1* and ceRNAs of *C1ORF21* expression showed that the correlation coefficients were between  $-0.033$  and  $0.423$  (Figure 10d), and the correlation coefficient between *GS1-115G20.1* and *C1ORF21* was  $0.365$ ,  $p = 2.2E-16$ , which is much higher in LUAD,  $r = 0.468$ . The “custom prediction” function of miRDB database was used to predict miRNA targets of lncRNA *GS1-115G20.1*, and there were 27 miRNAs that might interact with *GS1-115G20.1* (Table S9). In addition, we also found low *GS1-115G20.1* expression in the high *DKK1* expression group (Figure 10e,f). However, we did not find any evidence of their direct interaction in public databases.



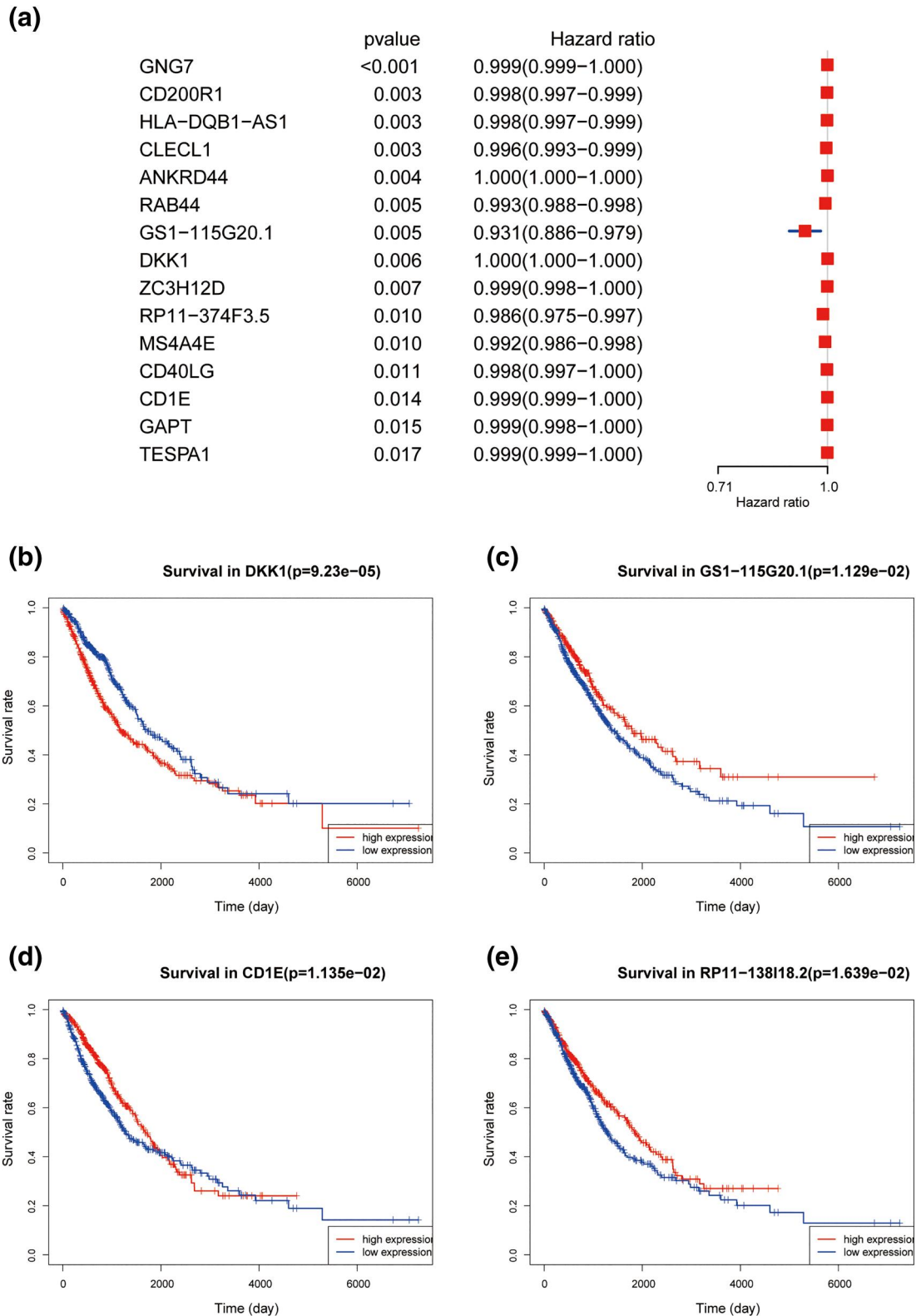


**FIGURE 5** Univariate regression analysis for screening prognostic genes. (a) Top 15 prognostic relevant genes in blue, light green and red modules of significance. (b, c, d, e): prognostic relevant genes were assigned into high and low expression groups based on median expression level, and the final Kaplan-Meier curves of four genes with  $p < 0.05$  were demonstrated. Kaplan-Meier curves of the *GS1-115G20.1* curve (c) divergence is obvious. *CD1E* curve (d) has a significant crossover and therefore is not significant

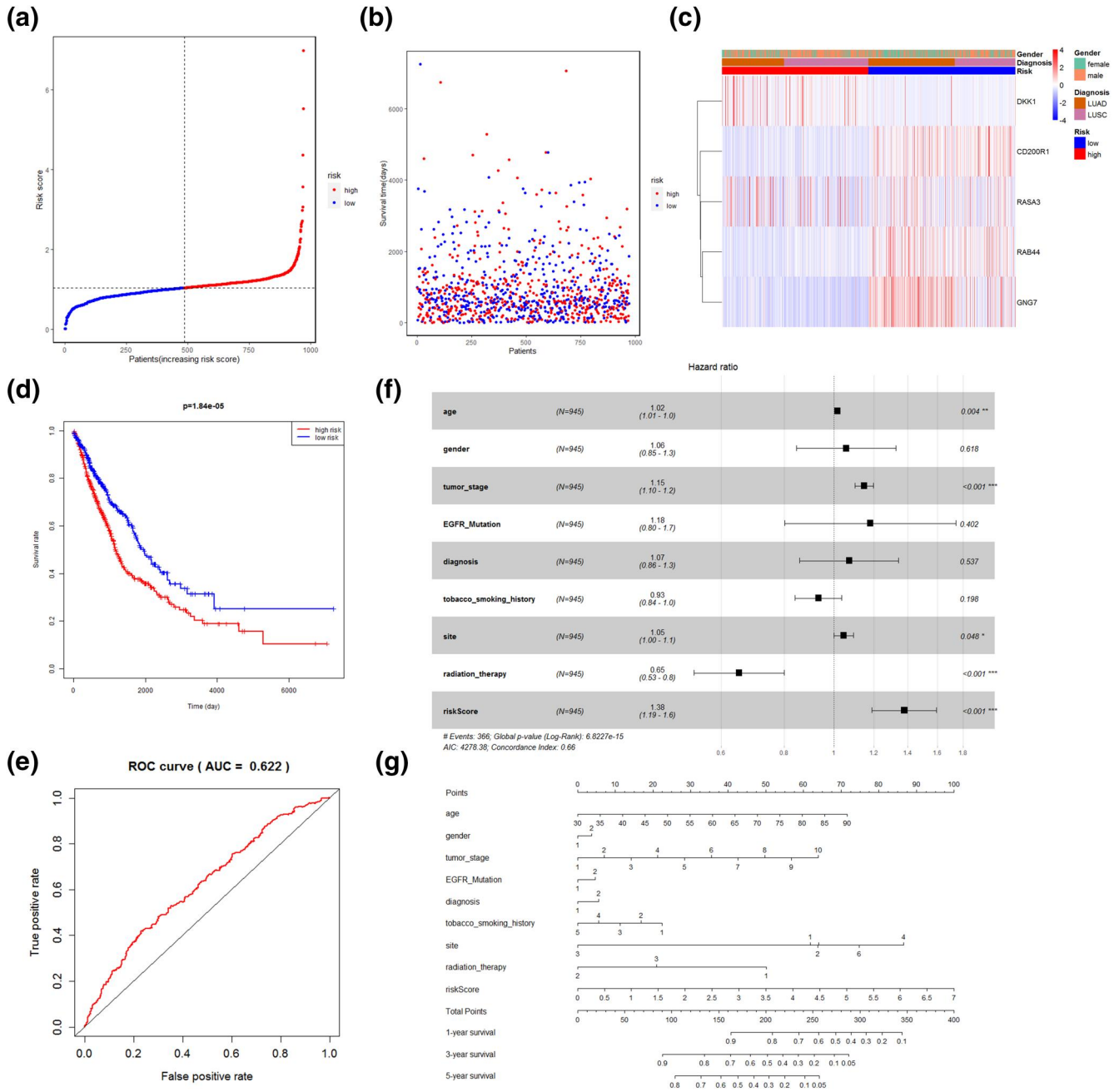


**FIGURE 6** Construction of the mRNA risk prognostic model. (a, b): Distribution of samples in high- and low-risk groups using median risk score one, with vertical coordinates of risk score one is shown. (c) Heat map shows the expression of five mRNA genes in the risk model in different risk score 1, different diagnoses, and different genders. (d) Kaplan-Meier curves for survival time of patients with high- and low risk. (e) ROC curves for predicting 3 year survival. (f) The forest plots of multivariate Cox regression. Black squares on the horizontal line indicate the hazard ratio and the horizontal lines show the 95% confidence interval. (g) Nomogram for predicting survival in NSCLC

## 4 | DISCUSSION

It has been proven that RYR mutations are frequently found in most cancer genomic studies with somatic mutations [6]. Nevertheless, the role and mechanism of RYR2 mutations in NSCLC pathogenesis and progression have not been confirmed. It is important to further clarify the potential genes related to the prognosis of NSCLC with RYR2 mutation. Extracting transcriptomic data from the UCSC Xena

dataset can help identify prognostic factors that may be involved in cancer development or evolution. In this study, we used genomic and transcriptomic data of LUAD and LUSC from the UCSC Xena database to identify lncRNAs and mRNAs, which are differentially expressed in RYR2 mutant and RYR2 wild-type NSCLC. By survival analysis, we found that patients in the RYR2 mutant group have better survival, and the somatic mutation of RYR2 may be protective.

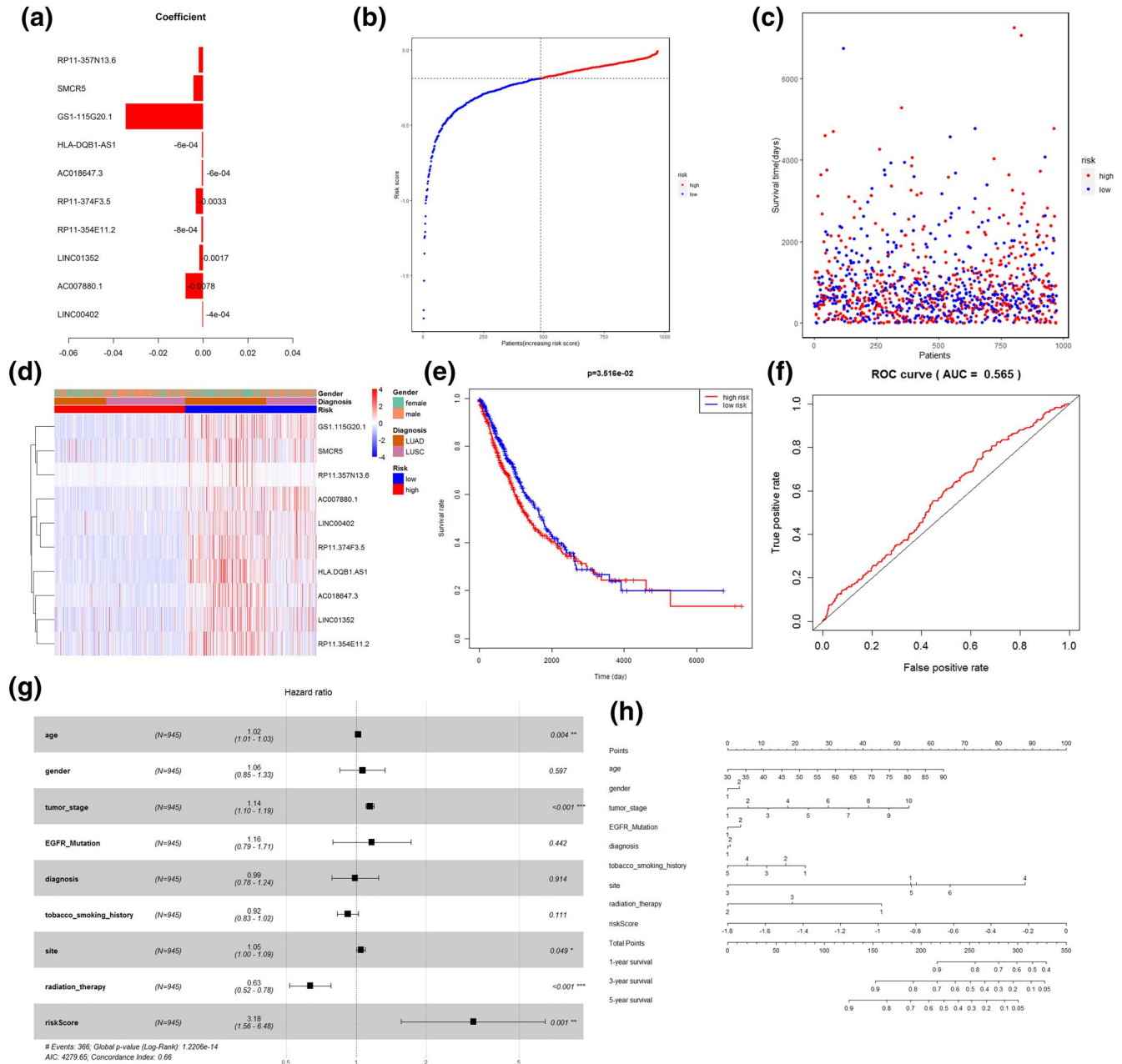


**FIGURE 7** Construction of the lncRNA risk-prognosis model. (a) 10 lncRNAs associated with prognosis and co-efficiency values. (b, c): Distribution of samples into high- and low-risk groups with median risk score 2 and vertical coordinates of Risk Score two is shown. (d) The risk model with 10 lncRNA genes expressed in different risk score two, different diagnoses, and different genders is shown in a heat map. (e) Survival curves of the high-risk and low-risk groups. (f) ROC curves for predicting 3 year survival. (g) The forest plots of multivariate Cox regression. Black squares on the horizontal line indicate the hazard ratio and the horizontal lines show the 95% confidence interval. (h) Nomogram for predicting survival in NSCLC

To further investigate the molecular mechanism by which *RYR2* mutation improves the prognosis of NSCLC patients, we constructed co-expression networks for DE mRNAs and DE lncRNAs, selected modules related to NSCLC prognosis for analysis, and constructed risk prognosis models for the prognosis-related mRNA and lncRNA genes. The important DE mRNA genes included were *RAB44*, *GNG7*, *RASA3*, *CD200R1* and *DKK1*. KEGG enrichment analysis showed that the DE mRNA gene was mainly related to neuroactive ligand-receptor interaction, complement and coagulation

casades, cAMP signalling pathway, adrenergic signalling in cardiomyocytes, cell cycle and other pathways. Among them, the cell cycle and cAMP signalling pathway are pivotal in tumour development in the study of NSCLC [33, 34]. Meanwhile, based on the above results, we constructed the mRNA risk prognostic model with reliable results for both internal and external validation. Although the transcriptome-based prognostic model has not yet reached a very satisfactory level for the prediction of survival in NSCLC patients, the attempt still has far-reaching implications.

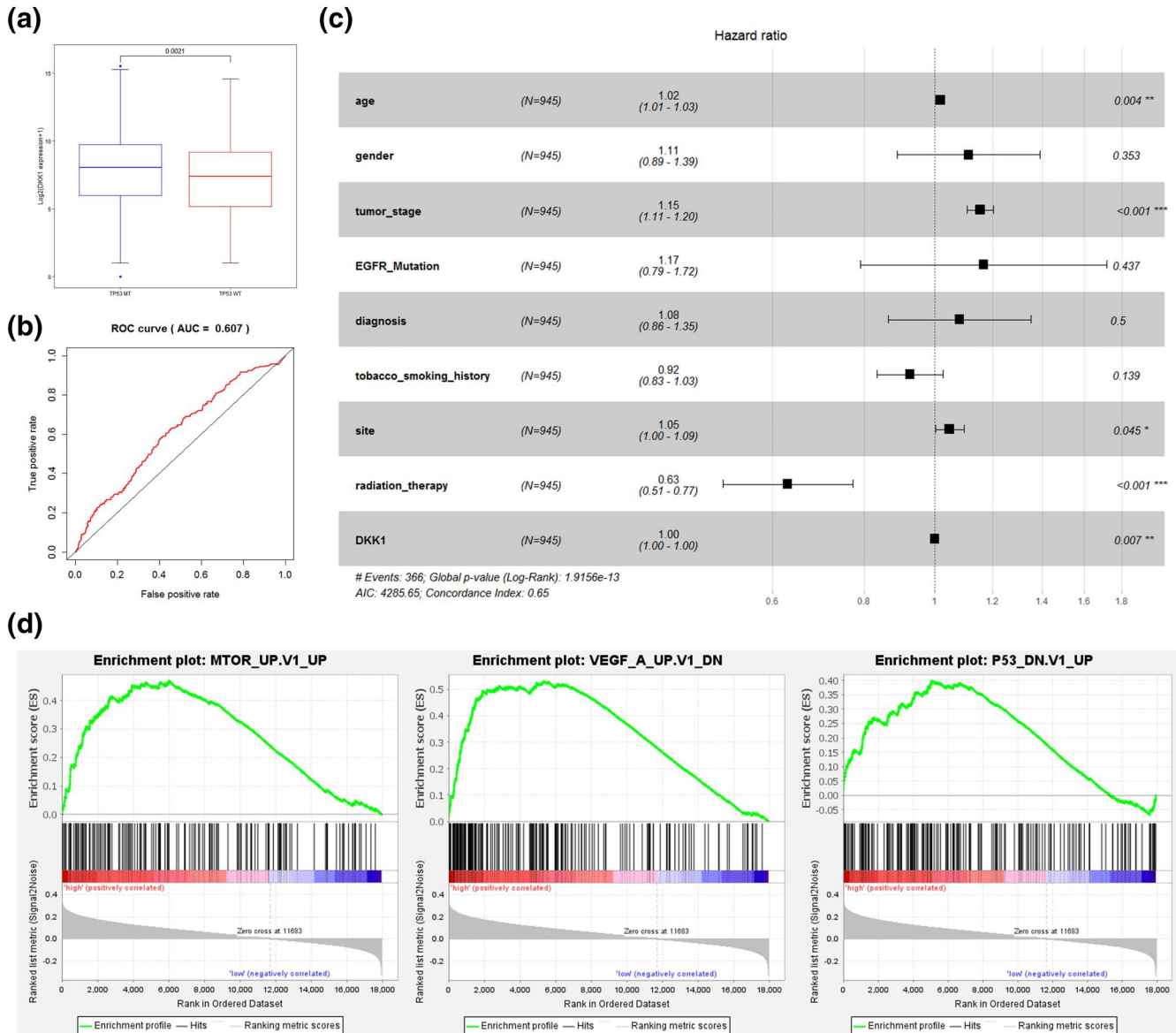


**FIGURE 8** *DKK1* is an independent prognostic factor. (a) *DKK1* was highly expressed in the *TP53* mutant group and low in the *TP53* wild group. (b) ROC curves of high and low *DKK1* expression predicting 3 year survival in NSCLC patients. (c) Multivariate Cox regression analysis with *DKK1* as an independent prognostic factor. (d) GSEA identified enrichment of *DKK1* low expression phenotype of the gene set

As the crucial DEmRNA gene in this study, the Dickkopf Wnt signalling pathway inhibitor-1 (*DKK1*) is a well-established classical Wnt signalling inhibitor [35], which is essential in the proliferation and migration of multiple tumour cell types [36]. Overexpressed *DKK1* promotes bony metastasis of breast cancer while inhibiting its lung metastasis, and even in the same tumours, an organ-specific role of *DKK1* has been noted [37]. Several studies have indicated associations of *DKK1* overexpression with cancer malignant progression and adverse prognosis in a raft of human cancers, suggesting a potential oncogenic function of *DKK1* [38–41]. Yamabuki et al. showed that high *DKK1* expression indicates adverse outcomes of NSCLC patients, and its exogenous expression improves migration and invasion of cells [40]. Notably, significant correlations between elevated serum *DKK1* protein concentrations

and tumour progression as well as lowered survival were identified in lung cancer patients [42]. In the results of this study, high *DKK1* mRNA expression in the *RYR2* wild type suggested a worse prognosis for lung cancer by analysing the UCSC xena database. In the present study, E47, CREL and AP1 were important cancer-related TFs enriched to *DKK1* high- and low-expressing DEmRNAs [43–45].

Recent advances have suggested that non-coding genes may also be new participants in the cancer paradigm [19]. In this study, a predictive model of lncRNAs was constructed, and in these lncRNAs, *GS1-115G20.1* may play a role in the development of NSCLC. *GS1-115G20.1* (also called *ENSG0000230470.1*; *OTTHUMG00000035468.1*; *AL078645.1*) is located on chromosome CHR1:184408336-184412360 (Grc h38), which is exactly located on the protein-coding gene

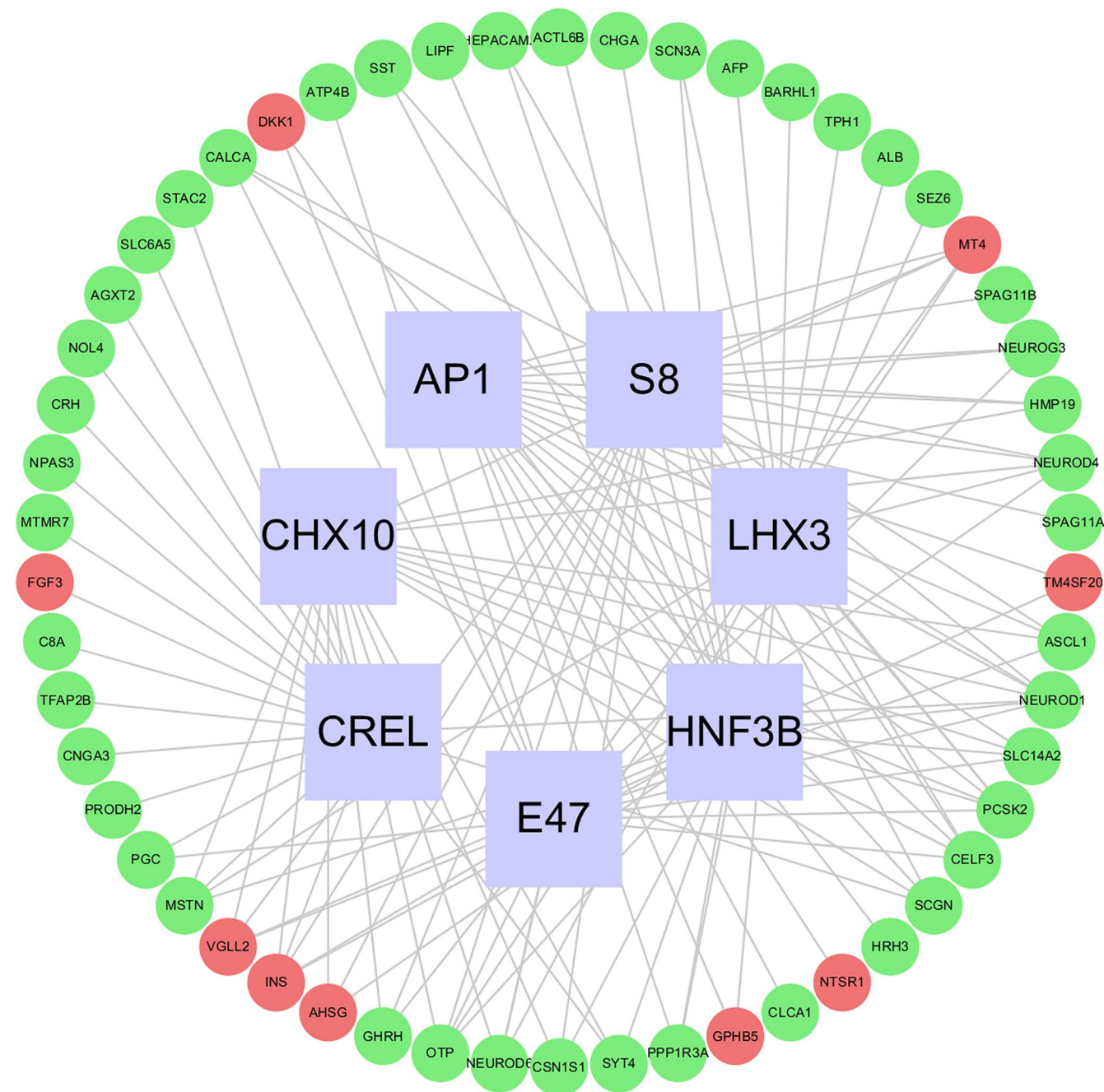


**FIGURE 9** The transcription factors regulatory network for DEmRNAs between high and low *DKK1* expression groups. The red genes are up-regulated, the green genes are down-regulated, and the blue boxes indicate the enriched transcription factors

*C1ORF21* (chr1:184387057-184629020) that encodes this protein gene [46]. The general regulatory effect of lncRNAs on adjacent mRNAs, coupled with expression correlation, leads to the speculation that *GS1-115G20.1* regulates the expression of *C1ORF21*, but the correlation is not strong. We found that the lncRNA's high expression in NSCLC indicated better survival and may play a protective function in NSCLC.

Due to the lack of experimental studies for *GS1-115G20.1*, we could only use predictive databases. As a result, several target miRNAs that may interact with *GS1-115G20.1* were identified (Table S8). hsa-miR-608 has been confirmed to play

a significant part in the apoptosis of NSCLC cells via the regulation of migration inhibitor factor (MIF), Akt serine/threonine kinase 2 (AKT2) and transcription factor activation enhancer binding protein 4 (TFAP4) [47–50]; Dong et al. found that hsa-miR-105-5p could be a biomarker for early diagnosis of NSCLC [51]; Zheng and other researchers found that hsa-miR-4651 elicited a negative effect on the progression of NSCLC via targeting bromodomain-containing protein 4 (BRD4) [52]; from a study by Wang's group, lncRNA LIFR-AS1 could inhibit NSCLC cell invasion and migration by serving as a sponge for hsa-miR-942-5p [53]; in patients

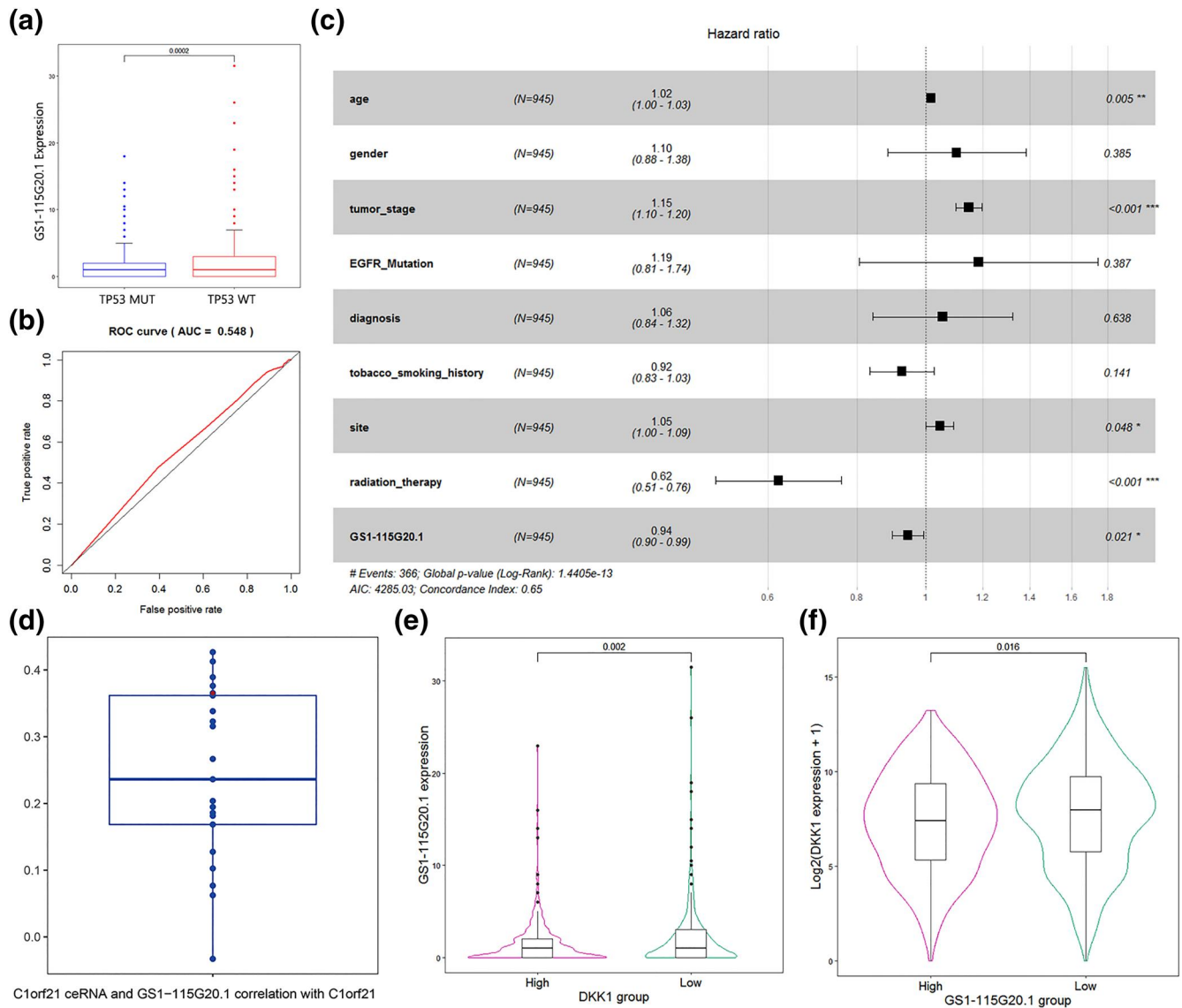


**FIGURE 10** *GSI-115G20.1* is an independent prognostic factor. (a) Low expression of *GSI-115G20.1* in the *TP53* mutant group and high expression of *GSI-115G20.1* in the *TP53* wild group. (b) ROC curves of high and low *GSI-115G20.1* expression to predict 3 year survival in NSCLC patients. (c) Results of multivariate Cox regression analysis with *GSI-115G20.1* as an independent prognostic factor. (d) Correlation analysis of ceRNAs of *C1ORF1*, *GSI-115G20.1* and *C1ORF21* expression. The red point in the graph is *GSI-115G20.1* ( $p = 2.2e-16$ ). (e) Expression changes of *GSI-115G20.1* at different *DKK1* expression levels. (f) Expression changes of *DKK1* at different *GSI-115G20.1* expression levels

suffering from anaplastic lymphoma kinase (ALK)-positive NSCLC, decreased hsa-miR-362-5p was accompanied by longer progression-free survival [54]. Therefore, we speculate that *GSI-115G20.1* may interact with the above miRNAs to have an influence on the phenotype, treatment, and prognosis of NSCLC, but further validation of molecular experiments is still needed.

In conclusion, using survival analysis, we found that *RYR2* mutations may have a protective effect on NSCLC. Through comprehensive bioinformatic analysis, two risk prognostic models of mRNA and lncRNA were established in this study, and prognostic risk models have some degree of predictive ability. The OS of high *DKK1* expression group and low *GSI-115G20.1* expression group was worse. Overall, our findings

may extend our understanding on the protective mechanisms of *RYR2* mutations on the prognosis of NSCLC and identify new targets for prognostic assessment and treatment.

#### ACKNOWLEDGEMENTS

We gratefully acknowledge the contributions of the TCGA Research Network (<https://www.cancer.gov/tcga>), UCSC Xena platform (<https://xenabrowser.net/>), KEGG (Kyoto Encyclopedia of Genes and Genomes), GO (Gene Ontology), DAVID (<https://david.ncifcrf.gov/home.jsp>), StarBase v2.0 (<http://starbase.sysu.edu.cn/starbase2/>) and miRDB (<http://mirdb.org/>). This study was sponsored by these projects: the Applied Basic Research Project of Yunnan Provincial Science and Technology Department and Kunming Medical University

(grant No. 2020001AY070001-117, 202001AY070001-130 and 202001AY070001-284); the Open Project of The First People's Hospital of Yunnan Province Clinical Medicine Center (2021LCZXXF-XZ03).

## CONFLICT OF INTEREST

The authors declare no conflict of interests.

## PATIENT CONSENT STATEMENT

Not applicable.

## DATA AVAILABILITY STATEMENT

All data, models, or codes that are generated in this study could be available upon reasonable request to the corresponding author.

## ORCID

Wenjun Ren  <https://orcid.org/0000-0002-9748-2960>

## REFERENCES

- Bray, F., et al.: Global cancer statistics 2018: GLOBOCAN estimates of incidence and mortality worldwide for 36 cancers in 185 countries. *CA Cancer J. Clin.* 68(6), 394–424 (2018)
- Yang, C.Y., Yang, J.C., Yang, P.C.: Precision management of advanced Non-Small cell lung cancer. *Annu. Rev. Med.* 71, 117–136 (2020)
- Howlader, N., et al.: SEER cancer statistics review, 1975–2016. Accessed 26 May (2019). [https://seer.cancer.gov/csr/1975\\_2016/2019](https://seer.cancer.gov/csr/1975_2016/2019)
- Inamura, K.: Adjuvant chemotherapy in patients with early-stage non-small cell lung cancer. *JAMA Oncol.* 4(7), 637–638 (2021)
- Zhang, X., Chang, A.: Somatic mutations of the epidermal growth factor receptor and non-small-cell lung cancer. *J. Med. Genet.* 44(3), 166–172 (2007)
- Schmitt, K., et al.: Somatic mutations and promotor methylation of the ryanodine receptor 2 is a common event in the pathogenesis of head and neck cancer. *Int. J. Cancer.* 145(12), 3299–3310 (2019)
- Shi, J., et al.: Pathological and prognostic indications of the mdig gene in human lung cancer. *Cell Physiol. Biochem.* 55(S2), 13–28 (2021)
- Yu, P., et al.: High expression of the SH3TC2-DT/SH3TC2 gene pair associated with FLT3 mutation and poor survival in acute myeloid leukemia: an integrated TCGA analysis. *Front. Oncol.* 10, 829 (2020)
- Van Petegem, F.: Ryanodine receptors: structure and function. *J. Biol. Chem.* 287(38), 31624–31632 (2012)
- Betzenhauser, M.J., Marks, A.R.: Ryanodine receptor channelopathies. *Pflugers Arch.* 460(2), 467–480 (2010)
- Thomas, N.L., et al.: Ryanodine receptor mutations in arrhythmia: the continuing mystery of channel dysfunction. *FEBS Lett.* 584(10), 2153–2160 (2010)
- Liu, Z., et al.: Association of RYR2 mutation with tumor mutation burden, prognosis, and antitumor immunity in patients with esophageal adenocarcinoma. *Front. Genet.* 12, 669694 (2021)
- Wei, Y., et al.: Impact of NR5A2 and RYR2 3'UTR polymorphisms on the risk of breast cancer in a Chinese Han population. *Breast Cancer Res. Treat.* 183(1), 1–8 (2020)
- Esteller, M.: Non-coding RNAs in human disease. *Nat. Rev. Genet.* 12(12), 861–874 (2011)
- Guttman, M., et al.: Ribosome profiling provides evidence that large noncoding RNAs do not encode proteins. *Cell.* 154(1), 240–251 (2013)
- Zhang, X., et al.: The role of long noncoding RNA in major human disease. *Bioorg Chem.* 92, 103214 (2019)
- Huarte, M.: The emerging role of lncRNAs in cancer. *Nat. Med.* 21(11), 1253–1261 (2015)
- Yang, X., et al.: High expression of lncRNA GACAT3 inhibits invasion and metastasis of non-small cell lung cancer to enhance the effect of radiotherapy. *Eur. Rev. Med. Pharmacol. Sci.* 22(5), 1315–1322 (2018)
- Shi, X., et al.: A critical role for the long non-coding RNA GAS5 in proliferation and apoptosis in non-small-cell lung cancer. *Mol. Carcinog.* 54(Suppl 1), E1–E12 (2015)
- Koboldt, D.C., et al.: VarScan 2: somatic mutation and copy number alteration discovery in cancer by exome sequencing. *Genome Res.* 22(3), 568–576 (2012)
- Robinson, M.D., McCarthy, D.J., Smyth, G.K.: edgeR: a Bioconductor package for differential expression analysis of digital gene expression data. *Bioinformatics.* 26(1), 139–140 (2010)
- McCarthy, D.J., Chen, Y., Smyth, G.K.: Differential expression analysis of multifactor RNA-Seq experiments with respect to biological variation. *Nucleic Acids Res.* 40(10), 4288–4297 (2012)
- GOC: The gene ontology resource: 20 years and still GOing strong. *Nucleic Acids Res.* 47(D1), D330–D338 (2019)
- Kanehisa, M., et al.: KEGG: new perspectives on genomes, pathways, diseases and drugs. *Nucleic Acids Res.* 45(D1), D353–D361 (2017)
- Iancu, O.D., et al.: Cosplicing network analysis of mammalian brain RNA-Seq data utilising WGCNA and Mantel correlations. *Front. Genet.* 6, 174 (2015)
- Langfelder, P., Horvath, S.: WGCNA: an R package for weighted correlation network analysis. *BMC Bioinforma.* 9, 559 (2008)
- Fuller, T.F., et al.: Weighted gene coexpression network analysis strategies applied to mouse weight. *Mamm. Genome.* 18(6–7), 463–472 (2007)
- Chen, J., et al.: Genomic landscape of lung adenocarcinoma in East Asians. *Nat. Genet.* 52(2), 177–186 (2020)
- Subramanian, A., et al.: Gene set enrichment analysis: a knowledge-based approach for interpreting genome-wide expression profiles. *Proc. Natl. Acad. Sci. U. S. A.* 102(43), 15545–15550 (2005)
- Huang, D.W., et al.: DAVID Bioinformatics Resources: expanded annotation database and novel algorithms to better extract biology from large gene lists. *Nucleic Acids Res.* 35(2), W169–W175 (2007)
- Li, J.H., et al.: StarBase v2.0: decoding miRNA-ceRNA, miRNA-ncRNA and protein-RNA interaction networks from large-scale CLIP-Seq data. *Nucleic Acids Res.* 42, D92–D97 (2014)
- Chen, Y., Wang, X.: miRDB: an online database for prediction of functional microRNA targets. *Nucleic Acids Res.* 48(D1), D127–D131 (2020)
- Chen, Z., et al.: CAMP/CREB-regulated LINC00473 marks LKB1-inactivated lung cancer and mediates tumor growth. *J. Clin. Invest.* 126(6), 2267–2279 (2016)
- Concato, V.M., et al.: 3,3',5,5'-tetramethoxybiphenyl-4,4'-diol induces cell cycle arrest in G2/M phase and apoptosis in human non-small cell lung cancer A549 cells. *Chem. Biol. Interact.* 326, 109133 (2020)
- Bafico, A., et al.: Novel mechanism of Wnt signalling inhibition mediated by Dickkopf-1 interaction with LRP6/Arrow. *Nat. Cell Biol.* 3(7), 683–686 (2001)
- Liu, Y., et al.: Prognostic significance of dickkopf-1 overexpression in solid tumors: a meta-analysis. *Tumour Biol.* 35(4), 3145–3154 (2014)
- Zhuang, X., et al.: Differential effects on lung and bone metastasis of breast cancer by Wnt signalling inhibitor DKK1. *Nat. Cell Biol.* 19(10), 1274–1285 (2017)
- Forget, M., et al.: The Wnt pathway regulator DKK1 is preferentially expressed in hormone-resistant breast tumours and in some common cancer types. *Br. J. Cancer.* 96(4), 646–653 (2007)
- Takahashi, N., et al.: Dickkopf-1 is overexpressed in human pancreatic ductal adenocarcinoma cells and is involved in invasive growth. *Int. J. Cancer.* 126(7), 1611–1620 (2009)
- Yamabuki, T., et al.: Dickkopf-1 as a novel serologic and prognostic biomarker for lung and esophageal carcinomas. *Cancer Res.* 67(6), 2517–2525 (2007)
- Yu, B., et al.: Elevated expression of DKK1 is associated with cytoplasmic/nuclear  $\beta$ -catenin accumulation and poor prognosis in hepatocellular carcinomas. *J. Hepatol.* 50(5), 948–957 (2009)

42. Sheng, S.L.E., et al.: Clinical significance and prognostic value of serum dickkopf-1 concentrations in patients with lung cancer. *Clin. Chem.* 55(9), 1656–1664 (2009)
43. Hunter, J.E., Leslie, J., Perkins, N.D.: C-Rel and its many roles in cancer: an old story with new twists. *Br. J. Cancer.* 114(1), 1–6 (2016)
44. Ibrahim, S.A.E., et al.: The role of AP-1 in self-sufficient proliferation and migration of cancer cells and its potential impact on an autocrine/paracrine loop. *Oncotarget.* 9(76), 34259–34278 (2018)
45. Zhu, G., et al.: PAK5-mediated E47 phosphorylation promotes epithelial–mesenchymal transition and metastasis of colon cancer. *Oncogene.* 35(15), 1943–1954 (2016)
46. Ronchetti, D., et al.: A compendium of long non-coding RNAs transcriptional fingerprint in multiple myeloma. *Sci. Rep.* 8(1), 6557 (2018)
47. Othman, N., Nagoor, N.H.: MiR-608 regulates apoptosis in human lung adenocarcinoma via regulation of AKT2. *Int. J. Oncol.* 51(6), 1757–1764 (2017)
48. Wang, Y., et al.: MicroRNA-608 promotes apoptosis in Non-Small cell lung cancer cells treated with doxorubicin through the inhibition of TFAP4. *Front. Genet.* 10, 809 (2019)
49. Yu, H.X., et al.: MiR-608 exerts tumor suppressive function in lung adenocarcinoma by directly targeting MIF. *Eur. Rev. Med. Pharmacol. Sci.* 22(15), 4908–4916 (2018)
50. Zhang, N., et al.: MiR-608 and miR-4513 significantly contribute to the prognosis of lung adenocarcinoma treated with EGFR-TKIs. *Lab. Invest.* 99(4), 568–576 (2019)
51. Dong, X., et al.: PlasmamiR-1247-5p, miR-301b-3p and miR-105-5p as potential biomarkers for early diagnosis of non-small cell lung cancer. *Thorac. Cancer.* 12(4), 539–548 (2021)
52. Zheng, J., et al.: MicroRNA-4651 targets bromodomain-containing protein 4 to inhibit non-small cell lung cancer cell progression. *Cancer Lett.* 476, 129–139 (2020)
53. Wang, Q., et al.: LncRNA LIFR-AS1 suppresses invasion and metastasis of non-small cell lung cancer via the miR-942-5p/ZNF471 axis. *Cancer Cell Int.* 20(1), 180 (2020)
54. Li, L., et al.: Circulating microRNAs as novel biomarkers of ALK-positive non-small cell lung cancer and predictors of response to crizotinib therapy. *Oncotarget.* 8(28), 45399–45414 (2017)

## SUPPORTING INFORMATION

Additional supporting information may be found in the online version of the article at the publisher's website.

**How to cite this article:** Ren, W., et al.: *RYR2* mutation in non-small cell lung cancer prolongs survival via down-regulation of *DKK1* and up-regulation of *GS1-115G20.1*: a weighted gene Co-expression network analysis and risk prognostic models. *IET Syst. Biol.* 16(2), 43–58 (2022). <https://doi.org/10.1049/syb2.12038>